Available online at www.sciencedirect.com
SCIENCE DIRECT
International Journal of Heat and Mass Transfer 49 (2006) 78–88
International Journal of HEAT and MASS TRANSFER
www.elsevier.com/locate/ijhmt

Experimental study of forced convection in asymmetrically heated sintered porous channels with/without periodic baffles

Sheng-Chung Tzeng [a,*], Tzer-Ming Jeng [b], Yen-Chan Wang [a]

[a] Department of Mechanical Engineering, Chienkuo Technology University, No. 1, Chieh Shou N Rd., Chang Hua 500, Taiwan, ROC
[b] Department of Mechanical Engineering, Air Force Institute of Technology, GangShan 820, Taiwan, ROC

Received 31 January 2005; received in revised form 5 August 2005
Available online 5 October 2005

Abstract

This study experimentally determined the local and average heat transfer characteristics in asymmetrically heated sintered porous channels with metallic baffles. The fluid medium was air. Measurements on the test specimen of four modes, without baffles (A), with periodic baffles on the top portion (B), with periodic baffles on the bottom portion (C) and with staggered periodic baffles on both sides (D), are performed. The effect of the average bead diameter was also examined ($d = 0.704$ and 1.163 mm). The data indicated that, the wall temperatures measured at baffles attached to the heated wall were slightly lower than those nearby, especially at high Reynolds numbers. In modes B and D, the heat transfer in the inlet region was weaker than that in modes A and C. Additionally, the heat transfer by forced convection in all modes increased as the bead diameter decreased. The effect of the bead diameter became stronger as the Reynolds number was increased. At $Re > 2000$, heat transfer was greatest in mode B and least in mode D, in which the heat transfer was even poorer than that without baffles. For a Re of around 1000, mode D was associated with an excellent heat transfer. In such a case, heat transfer enhancement was around $20 \sim 30\%$ in mode D, around $10 \sim 20\%$ in mode B and around $0 \sim 12\%$ in mode C.

Keywords: Sintered porous channels; Baffles; Forced convection

1. Introduction

Advances in modern electronics have led dramatic increases in the level of heat fluxes that must be removed to ensure the reliable operation of electronic packages. Conventional cooling methods that are based on forced convection are as follows: (1) Placing ribs periodically on the heat transfer surface disturbs the boundary layer. These ribs are small and do not disturb the core flow so most of the turbulence enhancement and boundary layer breakdown are localized near the heat transfer surface. (2) Inserting baffles into the heat transfer devices promotes mixing of the coolant. These baffles can significantly disturb the bulk flow. (3) Impingement cooling involves high velocity jets to cool directly the surface of interest. (4) Using heat sinks (such as fin arrays or porous media) increases the area in contact with the coolant. The extended dissipation area is widely

* Corresponding author. Tel.: +886 4 7111111x3132; fax: +886 4 7357193.
E-mail addresses: tsc@ctu.edu.tw, tsc33@ms32.hinet.net (S.-C. Tzeng).

0017-9310/$ - see front matter © 2005 Elsevier Ltd. All rights reserved.
doi:10.1016/j.ijheatmasstransfer.2005.08.006

Nomenclature

a, b	coefficients of empirical equation
d	average bead diameter, mm
F	inertial coefficient
H	channel height, mm
h	baffle height, mm
K	permeability, m^2
k	conductivity, W/m °C
L	channel length, mm
Nu	average Nusselt number, $Nu = \left(\sum_{i=1}^{n=13}(Nu_x \Delta x)_i\right)\Big/ n$
Nu_x	local Nusselt number, $qH/[(T_w - T_i)k_f]$
q	wall heat flux, W/m^2
Re	Reynolds number, $\rho_f UH/\mu$
T	temperature, °C
U	average fluid velocity in the x direction, m/s
w	baffle width, mm
x	coordinate, mm

Greek symbols

ε	porosity
μ	viscosity, kg/m s
ρ	density, kg/m^3

Superscript

—	average value

Subscripts

f	fluid
i	at channel inlet
s	solid
w	wall

recognized to improve the heat transfer. The combination of the aforementioned cooling methods, which should outperform any single method, will meet the future requirements of cooling designs.

Porous media have been extensively utilized in industrial applications, including electronic cooling, thermal energy absorption, geothermal systems and many others. They can present in the form of packed beds, sintered materials or foam materials. Many investigations of porous medium have been conducted [1–6]. However, the effective thermal conductivity of sintered porous media greatly exceeds that of non-sintered porous media because sintering causes thermal contact. Therefore, some researchers have focused on heat transfer behavior in sintered metallic particles. Hwang and Chao [7] measured the heat transfer in porous channels made of sintered bronze beads with two diameters, $d = 0.72$ mm and 1.59 mm. The fluid medium was air. Hwang et al. [8] provided a numerical model to simulate forced convection in an asymmetric heating sintered porous

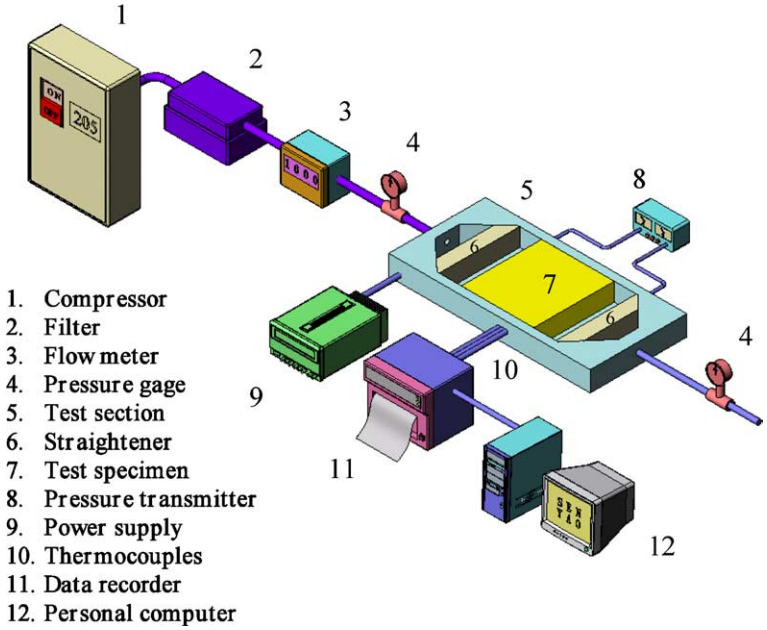

Fig. 1. Experimental apparatus.

channel. Their numerical model considered the non-Darcian effects of the no-slip boundary, flow inertia and thermal dispersion. The solid and the fluid phases were assumed to be in local thermal non-equilibrium. The local heat transfer coefficient at the inlet was determined by modified results for an impinging jet, and the non-insulated thermal condition was applied at the exit. Their numerical simulations agreed closely with the experimental results. Peterson and Chang [9] experimentally investigated two-phase dissipation in porous channels of various sizes filled with sintered copper particles. They found that the high thermal conductivity of the porous material and the large area of contact between the solid and the fluid together generate a highly effective, two-phase heat sink, which may provide an effective mechanism for cooling microelectronics with a high heat flux. Jiang et al. [10] also examined the heat transfer by forced convection in the sintered porous channels. The parameters varied in their experiments were fluid velocity, particle diameter of sintered bronze material ($d = 0.6$, 1.2 and 1.7 mm), type of porous media (sintered or non-sintered) and type of fluid (air or water). They reported that the dissipation of sintered material was better than that of non-sintered material. The local heat transfer coefficients of the sintered porous channels were up to 15 times higher for water than for empty channels and 30 times higher for air. They also reported that particle diameter did not strongly affect the heat transfer by convection in the sintered porous channel. The experiments herein improve our knowledge of heat transfer by sintered metallic materials. However, few works have addressed the cooling of combined sintered metallic materials and solid ribs or baffles.

This work experimentally measured the local and average heat transfer characteristics in sintered porous channels with baffles. The working fluid medium was air in present study. Solid baffles were inserted periodically into the sintered metallic materials in four modes. The effect of the average bead diameter of the sintered metallic materials was also considered. The results can be used to improve the cooling performance of sintered metallic porous structures and to clarify the analytical model.

2. Experimental apparatus and test section

The experimental setup, as presented in Fig. 1, was divided into four major parts—(1) air supply system; (2) test section; (3) test specimens, and (4) data acquirement system. Firstly, the air compressor blew air into the air tank. Then, the air flowed through a filter to remove the oil, water and particles. Finally, the air entered the test section after it passed through the straightened. The air flow rate was controlled using a flow meter. The test section was made of 40 mm-thick Bakelite. The dimensions of the channel section were 50 mm × 10 mm. The channel was filled with test specimens of size 50 mm × 10 mm × 50 mm. A film heater was fixed on the inner surface of the top wall of the channel. The other walls of the channel were insulated. The test specimens were made of sintered bronze beads with periodic cavities produced by WEDM (wire electronic discharge

Table 1
Physical properties of the sintered bronze beads

Sample	1	2
Average bead diameter, d (mm)	0.704	1.163
Porosity, ε	0.37	0.39
Thermal conductivity, k_s^* (W/m °C)	10.73	10.45
Permeability, $K \times 10^9$ (m^2)	0.283	0.67
Inertial coefficient, F	0.239	0.171

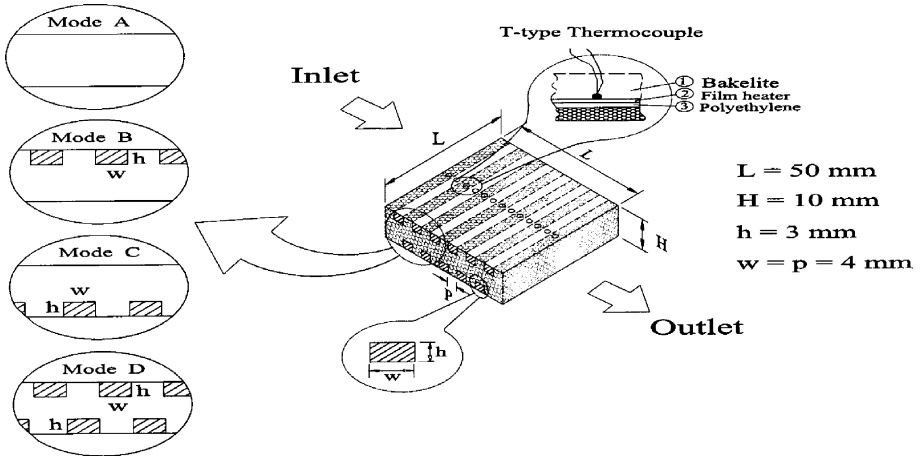

Fig. 2. Modes of test specimens and measured positions of thermocouples.

machine). Solid copper baffles were inserted into the cavities. The adequate amount of high-conductivity thermal grease was applied onto the contact surfaces among the film heater, sintered bronze beads and copper baffles to reduce the thermal contact resistance. The average diameters of the sintered bronze beads were 0.704 and 1.163 mm. Table 1 provides the relevant parameters associated with the porous properties, such as the permeability (K), the inertial coefficient (F), the effective solid conductivity (k_s^*), etc. The K and F values were determined by the method reported by Hunt and Tien [11]. The value of k_s^* was measured by performing a number of one-dimensional conduction heat transfer experiments and was employed for all the numerical tests. Note that the effective solid conductivity calculated using $k_s(1-\varepsilon)$, which is often used in the numerical study of heat transfer in porous media, is much higher than the experimental data. This phenomenon was also found by Jiang et al. [10]. The insertions of copper baffles of size 50 mm × 3 mm × 4 mm were divided into four modes. Mode A was without any baffle; mode B was with baffles periodically inserted into the top portion of the sintered bronze beads; mode C was with baffles periodically inserted into the bottom portion of the sintered bronze beads, and mode D was with baffles inserted periodically and in a staggered fashion into both the top and the bottom portions of the sintered bronze beads. Fig. 2 shows details of a typical test specimens studied herein. Thirteen T-type thermocouples were distributed on the centerline of the heated side. As depicted in Fig. 2, the temperatures of each baffle and the porous regions between baffles on the heated side were monitored. Three additional thermocouples were used to monitor the ambient temperature, the air temperature

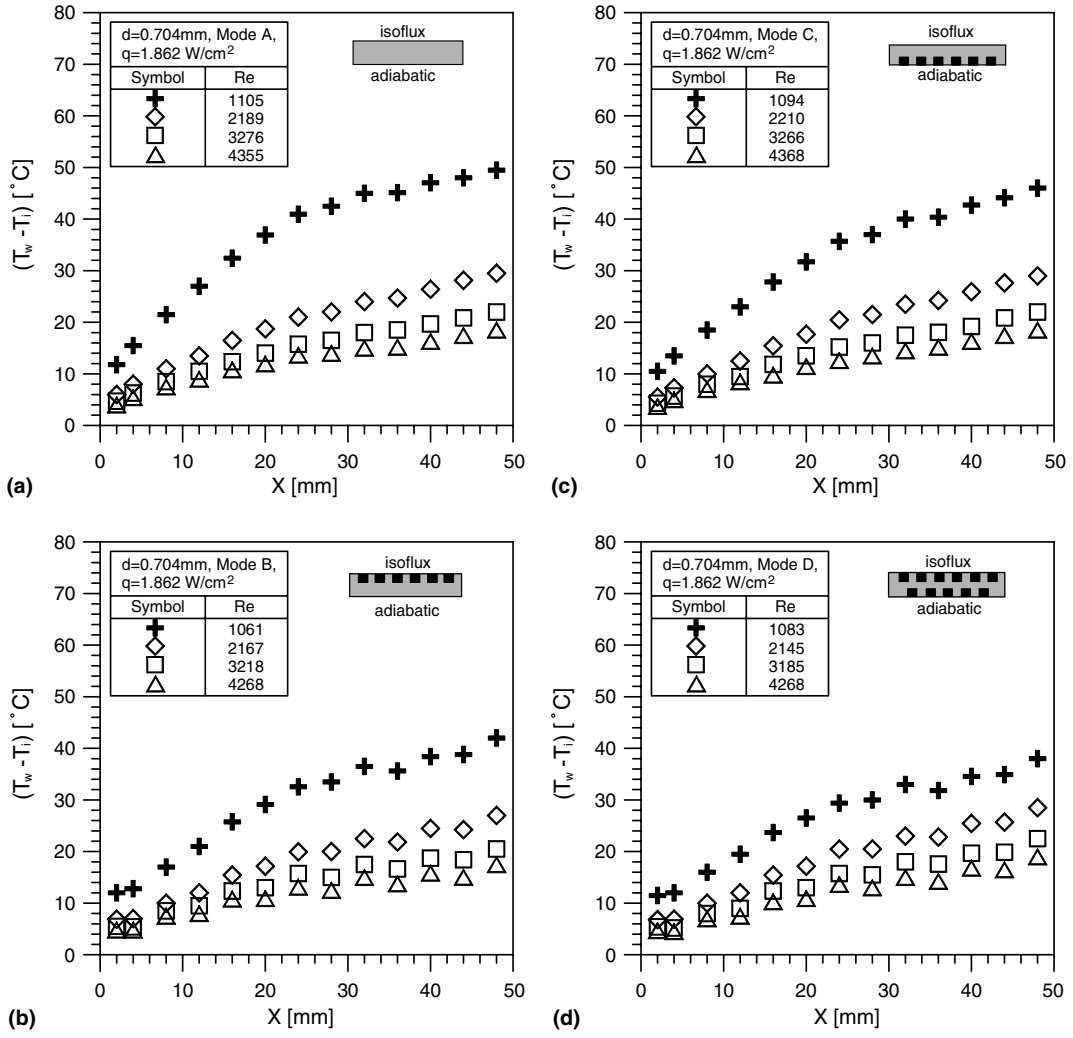

Fig. 3. Distributions of wall temperatures in x-direction for various Re and modes ($d = 0.704$ mm): (a) mode A, (b) mode B, (c) mode C, (d) mode D.

at the channel inlet and the air temperature at the channel outlet. A total of 16 thermocouples were connected to the data logger. The system was assumed to be in a steady state when the temperature did not vary by more than 0.2 °C during a 15 min interval. The pressure data at the channel inlet and the channel outlet were also obtained using pressure transmitters.

3. Data reduction and uncertainty analysis

The measured fluid velocities and temperatures were used to calculate the Reynolds numbers and the local and average Nusselt numbers, according to

$$Re = \frac{\rho_f UH}{\mu} \tag{1}$$

$$Nu_x = \frac{qH}{(T_w - T_i)k_f} \tag{2}$$

$$\overline{Nu} = \left(\sum_{i=1}^{13}(Nu_x \Delta x)_i\right) \Big/ L \tag{3}$$

The standard single-sample uncertainty analysis recommended by Kline and McClintock [13] and Moffat [14] was used. The experimental uncertainty in the flow rate was ±2.5%. The uncertainty in the pressure was 6.2%. The uncertainty in the temperature measurement was ±0.2 °C. The experimental uncertainty in the heat balance due to heat loss was ±6.7%. The experimental

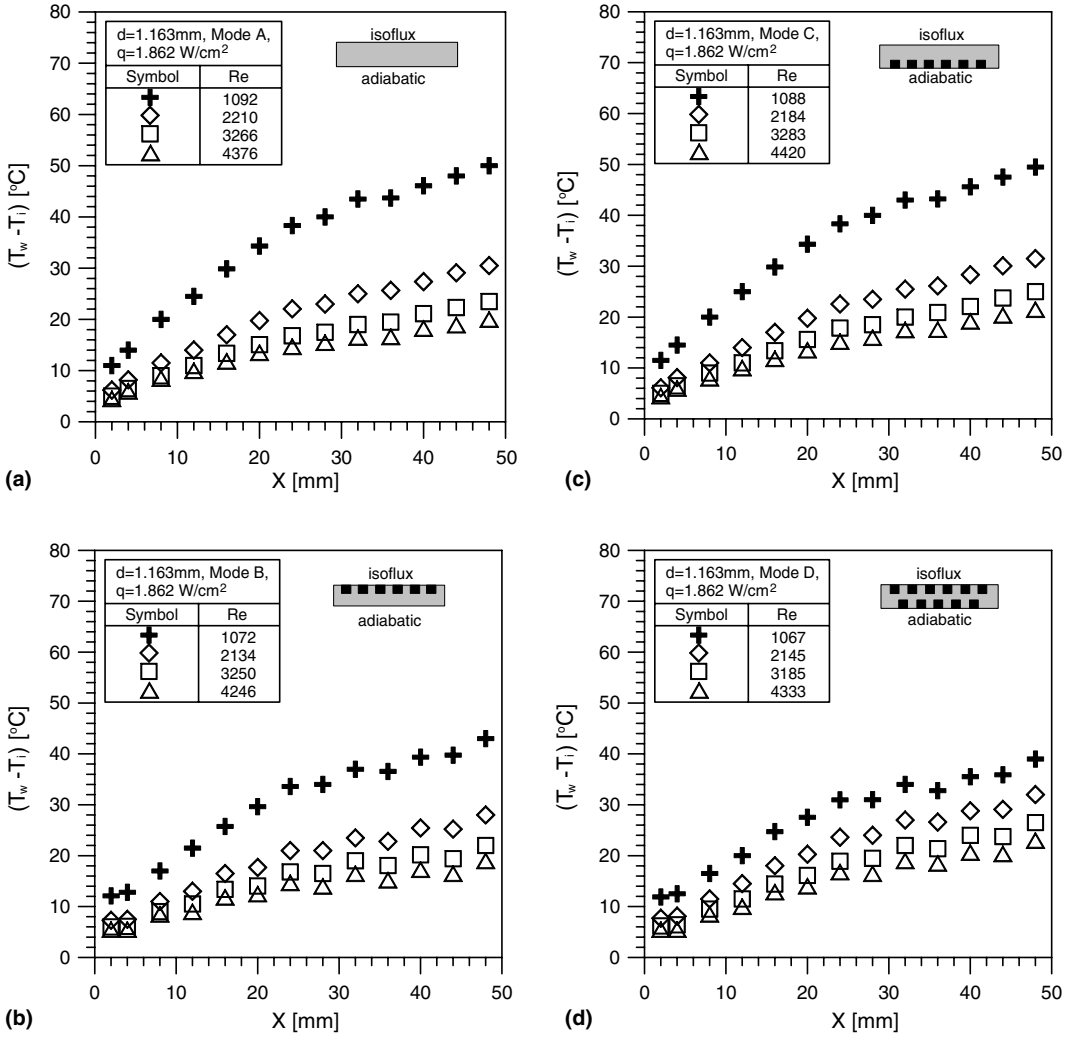

Fig. 4. Distributions of wall temperatures in x-direction for various Re and modes ($d = 1.163$ mm): (a) mode A, (b) mode B, (c) mode C, (d) mode D.

results herein revealed that the uncertainties in the Reynolds number and the Nusselt number were ±6.7% and ±7.1%, respectively.

4. Results and discussion

4.1. Distributions of wall temperature and validity of present experiments

Figs. 3 and 4 plot the heated wall temperature distributions in different modes in the x-direction at various Reynolds numbers and bead diameters. The figures reveal that for a given heat flux, the wall temperature increased with the axial distance, and declined as the Reynolds number increased. Additionally, when baffles were attached to the heated wall (as in modes B and D), the wall temperatures measured at the baffles were slightly lower than those at adjacent points, especially at large Reynolds numbers, because heat transfer at the baffles exceeded that at neighboring points. Fig. 5 compares the experimental data obtained in this work with other findings, to determine the validity of these tests. As far as the authors are aware, no experimental study has been conducted on heat transfer in sintered porous media inserted into metallic baffles. Therefore, only systems without baffles could be compared. Fig. 5(a) displays the experimental results of Hwang et al. [8], with a high level of consistency, and Fig. 5(b) presents the experimental results of Jiang et al. [10]. Because the effective thermal conductivity of sintered porous media in this work was about four times of that in the tests of Jiang et al. [10], the dimensionless parameter $h_{xb}H/(k_f^* + k_s^*)$ was used to ensure fair comparison of experimental results, where h_{xb} was the heat transfer coefficient determined from the bulk air temperature, and the data reduction method was that used by Jiang et al. [12]. In Fig. 5(b), it shows that the present work had a reasonable magnitude of $h_{xb}H/(k_f^* + k_s^*)$ by comparison with that of Jiang et al. [10].

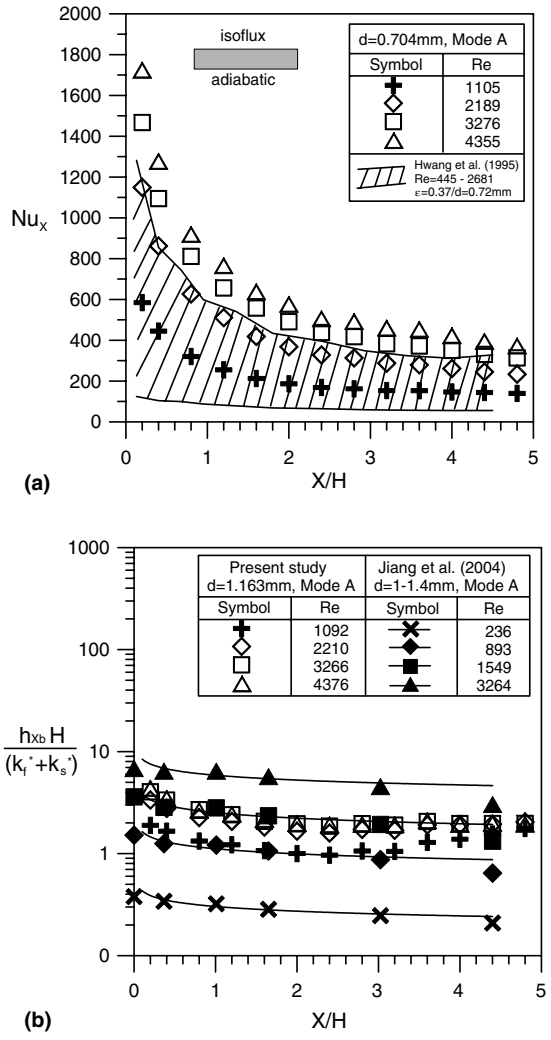

Fig. 5. Local heat transfer characteristics compared with others data. (a) Comparison with data of Hwang et al. [8]. (b) Comparison with data of Jiang et al. [10].

4.2. Effect of bead diameter on heat transfer

Fig. 6 shows the local Nusselt number distributions associated with different modes in the x-direction at various Reynolds numbers and bead diameters. The results reveal that, in modes B and D, the heat transfer performance in the inlet region was worse than that in modes A and C, because in the inlet region, the first baffle on the heated wall in modes B and D prevents the air from flowing near the heated wall. Fig. 6 also indicates that at high Reynolds numbers, the heat transfer by convection in all modes increased as the bead diameter declined. Jiang et al. [12] reported that the heat transfer coefficient of air increased as the diameter of non-sintered bronze particles decreased. The results in this work agree with those of Jiang et al. [12]. However, the effect of bead diameter on the heat transfer by convection was insignificant at the smaller Reynolds numbers studied herein. Fig. 7 plots the average Nusselt number versus Reynolds number in various modes and bead diameters. The data also indicates that the heat transfer by convection in all modes increased as the bead diameter declined. The bead diameter had a stronger effect as the Reynolds number was increased. The relationship between the average Nusselt number and the Reynolds number in the range studied herein was as follows:

$$\overline{Nu} = aRe^b \tag{4}$$

Table 2 presents the values of a and b in Eq. (4) for various bead diameters and modes, as determined by least

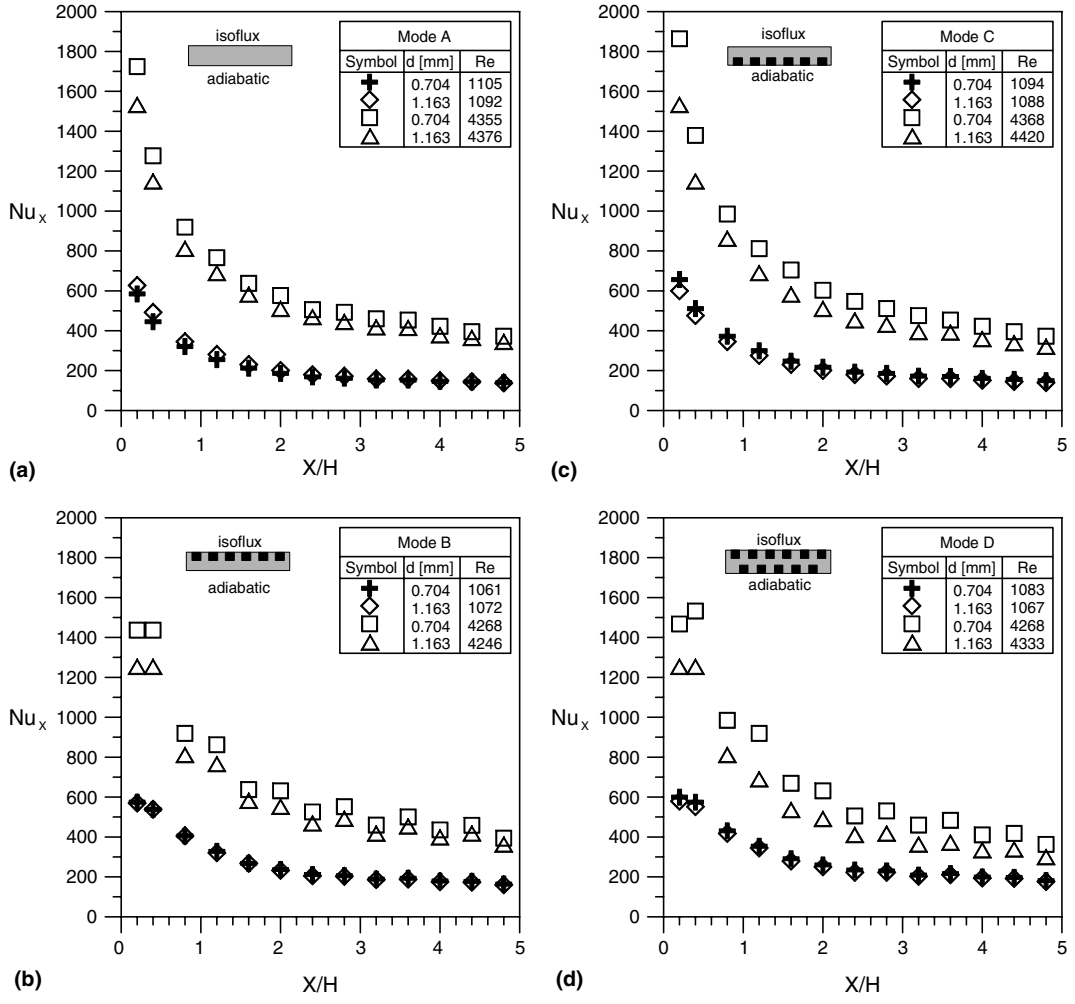

Fig. 6. Distributions of local Nusselt numbers in x-direction: (a) mode A, (b) mode B, (c) mode C, (d) mode D.

square analysis of the presented experimental data. The maximum deviation between Eq. (4) and the experimental data was under 5%.

4.3. Enhancement of heat transfer for porous media with periodically baffles

Figs. 8 and 9 compare local Nusselt numbers in mode A, indicating the increase in the local Nusselt numbers of porous media with baffles for various Reynolds numbers, bead diameters and modes. Due to the heat transfer at the baffles exceeded that at neighboring points, the oscillating patterns of local heat transfer enhancement for modes B and D in which baffles attached on the heated wall were presented. However, the oscillating patterns did not appear for mode C in which no baffle attached on the heated wall. Besides, the findings also reveal that, at $Re > 2000$, the heat transfer was most enhanced in mode B, and least enhanced in mode D, in which the heat transfer performance was even poorer than that without baffles. These differences among modes became significant as the bead diameter became larger. Additionally, for a Re of around 1000, the heat transfer was greatest in mode D, followed by mode B and then mode C. Inserting copper baffles into sintered porous media increased the complexity of the overall heat transfer mechanism. The possible benefits of copper baffles for heat transfer include, (1) increasing effective heating area; (2) increasing fin efficiency; (3) increasing flow turbulence, and (4) increasing local flow velocity in porous void. The first two benefits increase thermal conductivity through the solid matrix and heat can be transferred into the deep part of the porous channel comparing with the system without cooper baffles Ref. [15]. The latter two promote heat transfer coefficient between the fluid and the solid

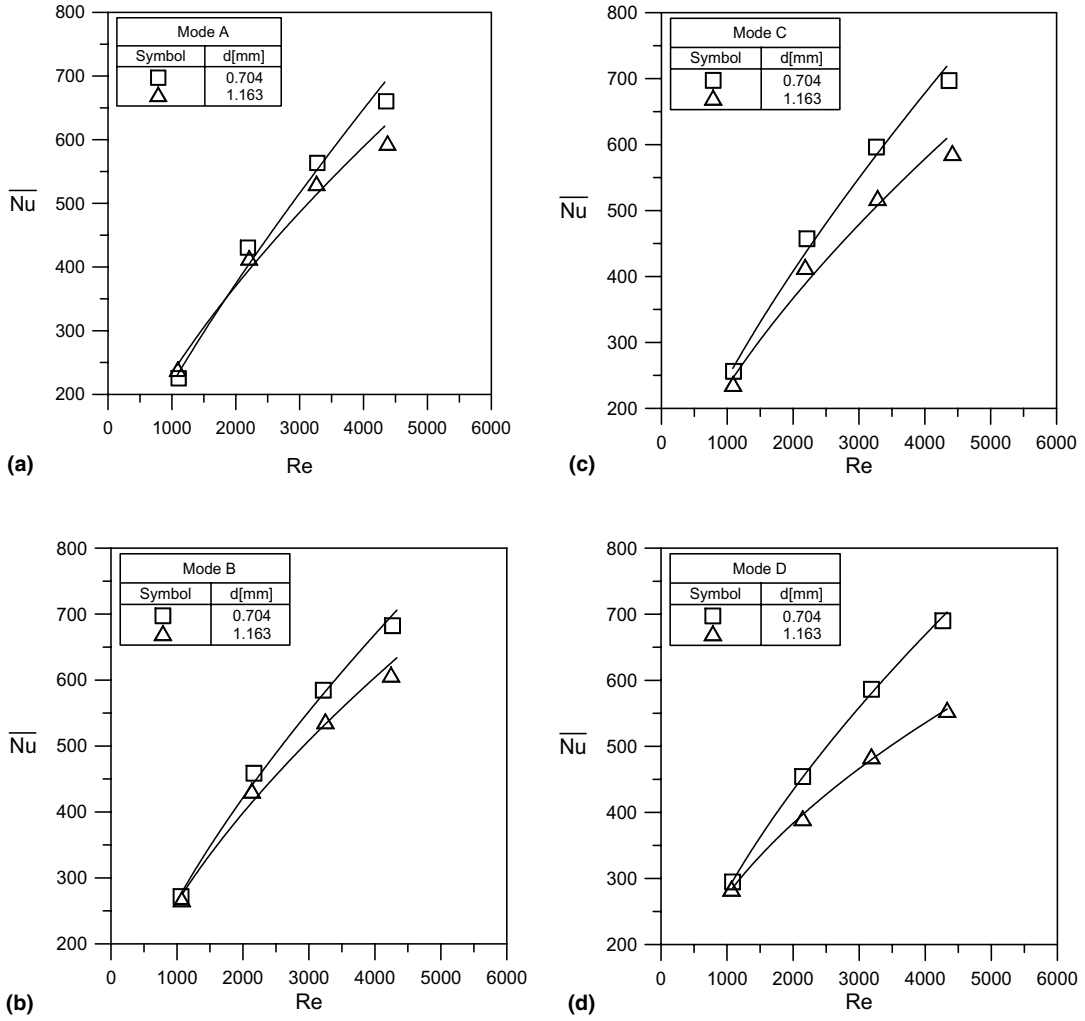

Fig. 7. Average Nusselt number as a function of Reynolds number—curve fit of the experimental data: (a) mode A, (b) mode B, (c) mode C, (d) mode D.

Table 2
The coefficient a and b of empirical equation for average Nusselt number

$\overline{Nu} = aRe^b$				
Average bead diameter	$d = 0.704$ mm		$d = 1.163$ mm	
Mode	a	b	a	b
A	0.908	0.792	2.289	0.669
B	2.656	0.667	4.184	0.599
C	1.57	0.732	2.519	0.655
D	3.763	0.625	9.923	0.481

matrix. The baffles also have some adverse effects on heat transfer, including, (1) reducing the volume of the porous media (i.e. reducing the effective dissipation area), and (2) preventing the coolant from flowing into the regions around neighboring baffles, especially when the flow is in a direction that allows it more easily to penetrate than it can in the cross direction (for example, when the particle or Reynolds number is large). This fact also accounts for the better heat transfer in mode D at small Re (for example, at $Re = 1000$), and the worse heat transfer at large Re (for example, at $Re > 2000$). Comparing the average Nusselt numbers in mode A, Figs. 10 and 11 reveal the enhancement in the average Nusselt numbers of porous media with baffles at various Reynolds numbers, bead diameters and modes. The results demonstrate that, at $Re > 2000$, sintered porous media with baffles insignificantly improved heat transfer, or exhibited heat transfer that was even poorer than that without baffles. However, at an Re of around 1000, heat transfer was enhanced by around

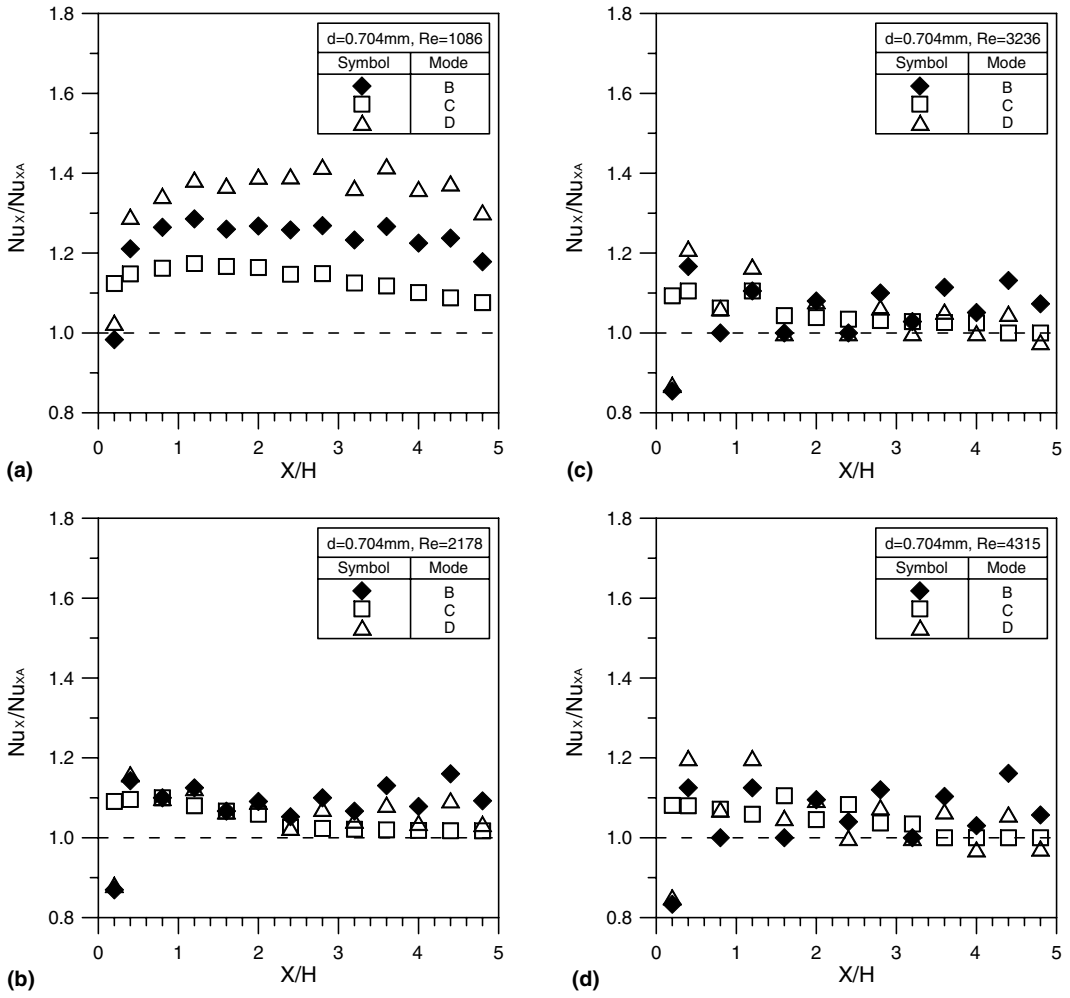

Fig. 8. Enhancements of local Nusselt numbers for porous media with baffles ($d = 0.704$ mm): (a) $Re = 1086$, (b) $Re = 2178$, (c) $Re = 3236$, (d) $Re = 4315$.

20–30% in mode D, around $10 \sim 20\%$ in mode B and around 0–12% in mode C.

5. Conclusion

This work experimentally measured the thermal characteristics of sintered porous channels with baffles. The solid baffles were inserted periodically into the sintered metallic materials in four modes. The effect of the bead diameter of sintered metallic materials was also examined. The following conclusions are drawn:

(1) At a given heat flux, the wall temperature increased with the the axial distance, and declined as the Reynolds number increased. Additionally, when baffles were attached on the heated wall (as in modes B and D), the wall temperatures measured at the baffles were slightly lower than those at the nearby points, especially at large Reynolds numbers.

(2) In modes B and D, the heat transfer in the inlet region was smaller than that in modes A and C because in the inlet region, the first baffle on the heated wall in modes B and D prevents the air from flowing near the heated wall.

(3) The heat transfer by convection in all modes increased as the bead diameter declined. The bead diameter had a stronger effect as the Reynolds number was increased.

(4) Generally, at $Re > 2000$, the heat transfer was enhanced in mode B, and worst in mode D, in which the heat transfer was even poorer than that without baffles. At an Re of about 1000, heat

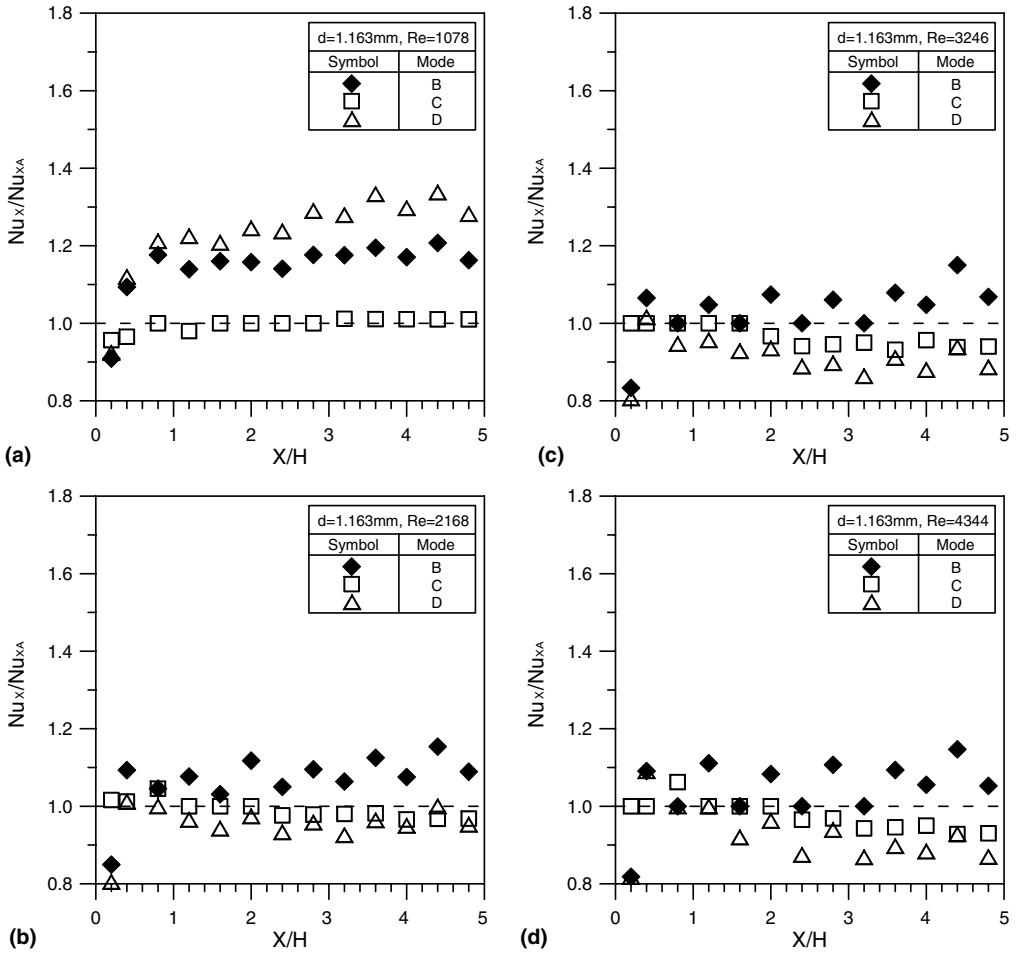

Fig. 9. Enhancements of local Nusselt numbers for porous media with baffles ($d = 1.163$ mm): (a) $Re = 1078$, (b) $Re = 2168$, (c) $Re = 3246$, (d) $Re = 4344$.

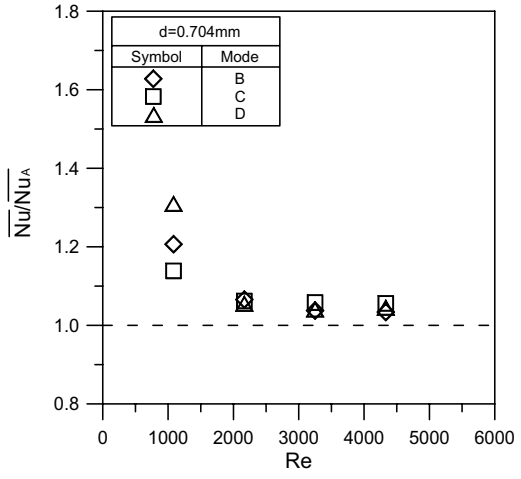

Fig. 10. Enhancements of average Nusselt numbers for porous media with baffles ($d = 0.704$ mm).

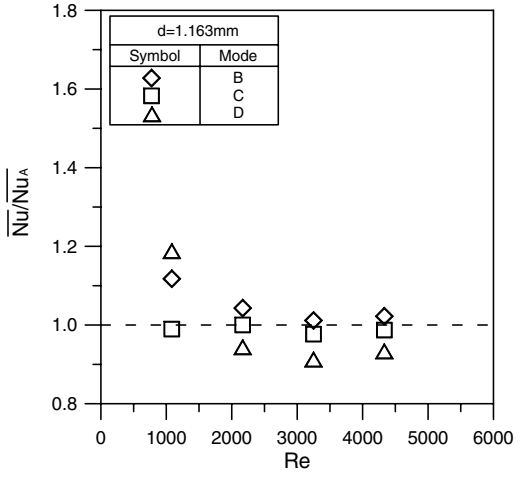

Fig. 11. Enhancements of average Nusselt numbers for porous media with baffles ($d = 1.163$ mm).

transfer was enhanced greatly in mode D. In this case, the heat transfer enhancement was around 20–30% in mode D, around 10–20% in mode B and around 0–12% in mode C.

(5) The relationship between the average Nusselt number and the Reynolds number, over the range studied here, was determined for various bead diameters and modes.

Acknowledgements

The authors would like to thank the National Science Council of the Republic of China for financially supporting this research under Contract No. NSC 92-2622-E-270-003-CC3.

References

[1] K. Vafai, M. Sozen, Analysis of energy and momentum transport for fluid flow through a porous bed, J. Heat Transfer 112 (1990) 690–699.
[2] M. Sozen, K. Vafai, Longitudinal heat dispersion in porous beds with real-gas flow, J. Thermophys. Heat Transfer (1993) 153–157.
[3] A. Amiri, K. Vafai, Analysis of dispersion effect and non-thermal equilibrium, non-Darcy variable porosity incompressible flow through porous media, Int. J. Heat Mass Transfer 37 (1994) 939–954.
[4] V.V. Calmidi, R.L. Mahajan, Forced convection in high porosity metal foams, J. Heat Transfer 122 (2000) 557–565.
[5] S.Y. Kim, B.H. Kang, J.H. Kim, Forced convection from aluminum foam materials in an asymmetrically heated channel, Int. J. Heat Mass Transfer 44 (2001) 1451–1454.
[6] K.C. Leong, L.W. Jin, Heat transfer of oscillating and steady flows in a channel filled with porous media, Int. Comm. Heat Mass Transfer 31 (2004) 63–72.
[7] G.J. Hwang, C.H. Chao, Heat transfer measurement and analysis for sintered porous channels, J. Heat Transfer 116 (1994) 456–464.
[8] G.J. Hwang, C.C. Wu, C.H. Chao, Investigation of non-Darcian forced convection in an asymmetrically heated sintered porous channel, J. Heat Transfer 117 (1995) 725–732.
[9] G.P. Peterson, C.S. Chang, Two-phase heat dissipation utilizing porous-channels of high-conductivity material, J. Heat Transfer 120 (1998) 243–252.
[10] P.X. Jiang, M. Li, T.J. Lu, L. Yu, Z.P. Ren, Experimental research on convection heat transfer in sintered porous plate channels, Int. J. Heat Mass Transfer 47 (2004) 2085–2096.
[11] M.L. Hunt, C.L. Tien, Effects of thermal dispersion on forced convection in fibrous media, Int. J. Heat Mass Transfer 31 (1988) 301–309.
[12] P.X. Jiang, Z. Wang, Z.P. Ren, B.X. Wang, Experimental research of fluid flow and convection heat transfer in plate channels filled with glass or metallic particles, Exp. Therm. Fluid Sci. 20 (1999) 45–54.
[13] S.J. Kline, F.A. Mcclintock, Describing uncertainties in single-sample experiments, Mech. Eng. (1953) 3–8.
[14] R.J. Moffat, Contributions to the theory of single-sample uncertainty analysis, ASME J. Fluid Eng. 104 (1986) 250–260.
[15] P.X. Jiang, R.N. Xu, M. Li, Experimental investigation of convection heat transfer in mini-fin structures and sintered porous media, J. Enhanc. Heat Transfer 11 (2004) 391–405.